

# **Serum neurofilament dynamics predicts neurodegeneration and clinical progression in presymptomatic Alzheimer's Disease**

Oliver Preische<sup>1,2,#</sup>, Stephanie A. Schultz<sup>3,#</sup>, Anja Apel<sup>1,2,#</sup>, Jens Kuhle<sup>4</sup>, Stephan A. Kaeser<sup>1,2</sup>, Christian Barro<sup>4</sup>, Susanne Gräber<sup>1</sup>, Elke Kuder-Buletta<sup>1</sup>, Christian LaFougere<sup>1</sup>, Christoph Laske<sup>1,2</sup>, Jonathan Vöglein<sup>5</sup>, Johannes Levin<sup>5</sup>, Colin L. Masters<sup>6</sup>, Ralph Martins<sup>7</sup>, Peter R. Schofield<sup>8</sup>, Martin N. Rossor<sup>9</sup>, Neill R. Graff-Radford<sup>10</sup>, Stephen Salloway<sup>11</sup>, Bernardino Ghetti<sup>12</sup>, John M. Ringman<sup>13</sup>, James M. Noble<sup>14</sup>, Jasmeer Chhatwal<sup>15</sup>, Alison M. Goate<sup>16</sup>, Tammie L.S. Benzinger<sup>3</sup>, John C. Morris<sup>3</sup>, Randall J. Bateman<sup>3</sup>, Guoqiao Wang<sup>3</sup>, Anne M. Fagan<sup>3</sup>, Eric M. McDade<sup>3</sup>, Brian A. Gordon<sup>3</sup>, Mathias Jucker<sup>1,2,\*</sup>, Dominantly Inherited Alzheimer Network

<sup>1</sup>DZNE-German Center for Neurodegenerative Diseases, Tübingen, Germany

<sup>2</sup>Department of Cellular Neurology, Hertie Institute for Clinical Brain Research, and Department of Psychiatry and Psychotherapy, University of Tübingen, Tübingen, Germany

<sup>3</sup>Department of Neurology, Department of Radiology, and Division of Biostatistics, Washington University School of Medicine, Saint Louis, MO, USA

<sup>4</sup>Neurologic Clinic and Policlinic, Departments of Medicine, Biomedicine and Clinical Research, University Hospital Basel, University of Basel, Basel, Switzerland

<sup>5</sup>DZNE-German Center for Neurodegenerative Diseases, Munich and Department of Neurology, Ludwig Maximilians University, Munich, Munich, Germany

<sup>6</sup>Neurodegeneration Division, The Florey Institute, University of Melbourne, Parkville, Victoria, Australia

<sup>7</sup>School of Medical Health and Sciences, Edith Cowan University and Department of Biomedical Sciences, Macquarie University, Australia

<sup>8</sup>Neuroscience Research Australia, Randwick, NSW 2031 and School of Medical Sciences, University of New South Wales, Sydney, NSW 2052, Australia

<sup>9</sup>Dementia Research Centre, Department of Neurodegeneration, Queen Square Institute of Neurology, University College London, London WC1N 3BG, U.K.

<sup>10</sup>Department of Neurology, Mayo Clinic Jacksonville, Jacksonville, FL, USA

<sup>11</sup>Alpert Medical School of Brown University, Providence, RI, USA

<sup>12</sup>Indiana Alzheimer Disease Center and Department of Pathology and Laboratory Medicine, Indiana University School of Medicine, Indianapolis, IN, USA

<sup>13</sup>Department of Neurology, Keck School of Medicine at USC, Los Angeles, CA, USA

<sup>14</sup>Taub Institute for Research on Alzheimer's Disease and the Aging Brain, Department of Neurology, Columbia University Medical Center, New York, NY, USA

<sup>15</sup>Department of Neurology, Massachusetts General Hospital, Harvard Medical School, Boston, MA, USA

<sup>16</sup>Department of Neuroscience, Icahn School of Medicine at Mount Sinai, New York, NY, USA

#contributed equally; \* corresponding author

**Neurofilament light chain (NfL) is a promising fluid biomarker of disease progression for various cerebral proteopathies. Here we leveraged the unique characteristics of the Dominantly Inherited Alzheimer Network (DIAN) and ultrasensitive immunoassay technology to demonstrate that NfL levels in CSF (n=187) and serum (n=405) are correlated with one another and are elevated at presymptomatic stages of familial Alzheimer's disease (AD). Longitudinal, within-person analysis of serum NfL dynamics (n=196) confirmed this elevation and further revealed that the rate of change of serum NfL could discriminate mutation carriers from non-mutation carriers almost a decade earlier than cross-sectional absolute NfL levels (i.e. 16.2 vs. 6.8 years before estimated symptom onset). Serum NfL rate of change peaked in participants converting from the presymptomatic to the symptomatic stage, and associated with cortical thinning assessed by MRI, but less so with amyloid- $\beta$  (A $\beta$ ) deposition or glucose metabolism (assessed by PET). Serum NfL was predictive for both the rate of cortical thinning and cognitive changes assessed by mini-mental state examination and logical memory testing. In conclusion, NfL dynamics in serum predicts disease progression and brain neurodegeneration at early presymptomatic stages of familial AD, which supports its potential utility as a clinically useful biomarker.**

In most neurodegenerative diseases, brain changes manifest many years before clinical symptoms become apparent. In AD, presymptomatic changes in brain include cortical thinning and neuropathological depositions containing A $\beta$  and tau. These pathological changes can be assessed by MRI, PET, and measurement of A $\beta$  and tau protein levels in CSF<sup>1-4</sup>. However, CSF collection and imaging modalities are invasive and expensive, respectively, and therefore not well suited to routine clinical practice. Blood biomarkers for the presymptomatic phase of AD are largely lacking, although recent progress in the analysis of A $\beta$ , tau, and NfL in blood have been reported<sup>5-10</sup>.

NfL is a component of the axonal cytoskeleton and is primarily expressed in large caliber myelinated axons<sup>11,12</sup>. Changes of NfL in bodily fluids have been linked to brain damage and brain atrophy in mouse models and multiple neurological disorders including proteopathic neurodegenerative diseases<sup>11,13-16</sup>. Advancements in NfL measurements revealed tight correlations between NfL in CSF and blood and have sparked interest in an NfL blood-based biomarker that monitors neurodegeneration and disease progression. However, longitudinal analyses are largely missing and the importance of NfL as a molecular biomarker for the presymptomatic phase of neurodegenerative diseases remains unclear<sup>6,9,17</sup>.

We made use of DIAN<sup>18</sup> data and biospecimens to study NfL changes in CSF and blood of presymptomatic and symptomatic AD. DIAN participants are members of families carrying highly penetrant autosomal-dominant mutations in the genes encoding the amyloid beta precursor protein (*APP*) or presenilin 1 or 2 (*PSEN1* and *PSEN2*)<sup>19</sup>. Family members who do not carry the mutations serve as controls. As the age of symptom onset tends to be consistent for a given mutation, it is possible to calculate for participants an estimated year to symptom onset (EYO) from the known onset of individuals with the same mutation<sup>20</sup>.

We used the single-molecule array immunoassay technology to measure NfL in CSF and blood serum of DIAN participants at their baseline (initial) visit (mutation carriers, MC: n=243; non-carriers, NC; n=162) (see Supplementary Table 1 for participant characteristics). Multivariate linear mixed-effects (LME) models served to assess the earliest point in the disease when NfL starts to increase in MC in relation to NC (Fig. 1a, b). Results revealed that NfL in CSF was significantly increased between MC and NC at -6.8 EYO (Fig. 1a, Extended Data Fig. 1a). Almost identically, serum NfL was also increased at -6.8 EYO (Fig. 1b; Extended Data Fig. 1b). Consistent with our earlier work<sup>13</sup> CSF and serum NfL levels were

tightly associated (Fig. 1c, d). No differences in CSF or serum NfL levels between the three familial AD mutations were found (Extended Data Fig. 2).

Given the strong association between serum and CSF NfL, and the obvious advantage of a non-invasive disease blood biomarker<sup>21</sup>, we chose to focus on serum NfL for subsequent longitudinal analyses. From the 405 participants with baseline serum, 196 participants returned for at least one and maximally 5 follow-up visits, with a mean number of 2.5 visits and a median observation time of 3 years from the baseline visit (see Supplementary Table 2 for longitudinal participant characteristics).

Overall, the longitudinal analysis of serum NfL confirmed the cross-sectional findings (Fig. 2a). Using LMEs we calculated the slope of NfL change per year for each participant. As with cross-sectional values, the NfL rates of change were significantly elevated in MC relative to NC. Strikingly, however, the first EYO point where this increase became significant was at -16.2 years (Fig. 2b; see also Extended Data Fig. 3), which is almost a decade earlier than the cross-sectional baseline estimates (-6.8 EYO, see above). Consistent with this earlier separation of MC and NC using longitudinal measurements, the rate of change was able to distinguish presymptomatic MC from NC more accurately compared to baseline serum NfL using Receiver Operating Characteristics (ROC) analysis (Extended Data Fig. 4).

Next, we subdivided MC into three groups: presymptomatic MC (individuals who scored “zero” on the Clinical Dementia Rating [CDR] across all visits), converters (CDR=0 at baseline and CDR>0 at subsequent visits) and symptomatic MC (CDR>0 across all visits). We then compared the rate of change in serum NfL across these groups. Analyses revealed that the rate of change in serum NfL peaked in the converter group with no further increase in the symptomatic carriers (Fig. 2c). Interestingly, flattening or even U-shaped curves have also been observed in longitudinal studies for CSF biomarkers in dominant and sporadic AD<sup>22,23</sup>.

No differences in NfL rate of change were found between mutations in *APP*, *PSEN1*, and *PSEN2* (Extended Data Fig. 5a). To analyze whether NfL rate of change was associated with the aggressiveness of individual mutations or EYO, we analyzed how far away the NfL rate of change of each MC was from the median value from the model estimates at that individual’s EYO (Extended Data Fig. 5b). Although we did not find any significant differences, it is possible that differences become apparent when the number of subjects and longitudinal data points increase.

To study if brain changes are coupled with changes in serum NfL, regression analysis between NfL rates of changes and rates of change in brain imaging modalities were performed. We focused on the precuneus as previous analyses have shown this area to be most sensitive to AD progression<sup>2,24</sup>. NfL rates of change in serum and rates of precuneus cortical thinning were significantly associated in symptomatic MC with a trend towards significance in presymptomatic MC (Fig. 3a). The rate of change in serum NfL and the rate of change in precuneus glucose metabolism (FDG-PET) were significantly associated in symptomatic MC but not in presymptomatic MC (Fig. 3b). Although there was a positive relationship between NfL rate of change and the rate of change in precuneus A $\beta$  deposition (A $\beta$ -PET), the association did not reach significance (Fig. 3c). These results indicate that NfL changes in blood most closely reflect cortical thinning and support the view that serum NfL is primarily a marker of neurodegeneration.

To examine the utility of serum NfL for predicting subsequent neurodegeneration and clinical symptoms, we performed a (retrospective) pseudo-predictive analysis to ask whether baseline serum NfL levels were predictive of subsequent cortical thinning (Fig. 4a). In addition, we assessed the predictability of baseline serum NfL for detecting change in two cognitive parameters, namely Mini-Mental State Examination (MMSE) and Logical Memory Test (Fig.

4b, c). Indeed, baseline NfL was highly predictive of future annualized cortical thinning (for both presymptomatic and symptomatic MC) at subsequent visits (Fig. 4a) and was also predictive for a decrease in MMSE and Logical Memory Scores (Fig. 4b, c).

To examine whether serum NfL is also predictive in a truly prospective design, the first 39 MC returning for follow-up visits after the last serum collection were included in the analysis (median time between last serum collection and subsequent visit was 2.1 years). This prospective analysis now allowed us to use the serum NfL rate of change for the prediction of further cortical thinning and cognitive changes (from the last visit with serum collection to the follow-up visit). Despite the small sample size, significant (predictive) associations were found between serum NfL rate of change and cortical thinning as well as MMSE and Logical Memory Test (Fig. 4d-f).

Cross-sectional and longitudinal data analyses of DIAN and other large AD cohorts have demonstrated that the pathologic processes in AD begin more than two decades before the onset of clinical symptoms. The accumulation of A $\beta$  in brain (estimated 15-20 years before clinical onset) is followed by declines in cortical metabolism (estimated 10-15 years before clinical onset) and brain atrophy (5-10 years before clinical onset)<sup>1,2,22,25</sup>. Thus it is generally agreed that therapeutic interventions should start as early as possible making disease biomarkers of the presymptomatic phase of utmost importance<sup>4,26</sup>. The present results suggest that NfL levels in blood may serve as such a biomarker to monitor neurodegeneration and disease progression already in presymptomatic AD.

The strong association between NfL levels in CSF and blood indicates that NfL changes in blood reflect changes in the brain, a finding also reported for other neurodegenerative diseases including sporadic AD<sup>6,13,27,28</sup>. In the present study serum was analyzed but similar levels and tight correlations have also been reported for NfL in plasma<sup>13,27</sup>. The antigen detected with the (ultrasensitive) immunoassay used in this study is presumably a short and stable fragment (~10 kD) of the core domain of NfL<sup>15,29</sup>. Such a stable fragment appears well suited as blood biomarker for monitoring a slow neurodegenerative process in brain.

Using serial NfL measurements we found that NfL annual rate of change can distinguish NC and MC as early as 16 years before estimated symptom onset. This is almost a decade earlier than when using absolute NfL levels measured at a single time point. Consistently, previous studies reported only non-significant or barely significant increases of absolute NfL in blood in presymptomatic or even mildly cognitive impaired AD patients<sup>6,9,13</sup>. In symptomatic AD, our results suggest the NfL rate of change reaches a plateau while absolute NfL levels continue to increase. Increased absolute NfL levels in blood in the symptomatic disease phase is consistent with similar observations in progressive supranuclear palsy<sup>28</sup>, Huntington disease<sup>30</sup> and multiple sclerosis<sup>14</sup>.

The very early changes of NfL in blood may appear surprising in light of the reported overall brain atrophy only 5-10 years before symptom onset. However, atrophy of individual cortical regions occur earlier<sup>1,2,22,25</sup>. In fact, precuneus thinning was also detected around 16 years before symptom onset<sup>2</sup>, suggesting that NfL changes are sensitive enough to pick up such early, regional brain atrophy. The association between NfL and cortical thinning, rather than A $\beta$  deposition, is in line with cerebral A $\beta$  aggregation being a trigger of subsequent neurodegeneration that, however, becomes independent of each other at later disease stages<sup>31</sup>. The relationship of NfL to Tau in bodily fluids needs further work. In the DIAN cohort, the increase of Tau in CSF (absolute levels, cross-sectional) occurs as early as 15 years before estimated age of symptom onset<sup>32</sup>, which is much earlier than the increase of baseline NfL in CSF.

While increase of NfL levels is not specific for AD, the present findings are relevant for understanding AD disease progression and highlight their utility as a marker in clinical trials. In presymptomatic AD, the greater the NfL rate of change, the closer an individual is to converting to symptomatic AD, a finding also reported for cortical atrophy<sup>2,33</sup>. This suggests that longitudinal measures of NfL in serum are a reliable, but relatively cheap and fast readout of neurodegeneration in the brain with comparable diagnostic value to neuroimaging but without the regional resolution.

Although our prospective predication analysis was not adequately powered to demonstrate that NfL rate of change is indeed a better predictor for disease progression (neurodegeneration and cognitive decline) than absolute NfL values, our observations suggest that this is the case in presymptomatic AD, while absolute NfL levels are better predictors in the symptomatic phase. Absolute NfL levels have been successfully used to predict brain volume changes in (symptomatic) multiple sclerosis<sup>14</sup> and clinical outcome in traumatic brain injury<sup>34</sup>. In a recent study with Huntington's disease patients NfL blood levels were predictive of disease onset within 3 years<sup>30</sup>, but NfL rate of change was not assessed.

The current study design with the 2-3 years-interval between participant assessments did not allow us to determine the relationship between the time over which NfL rate of change was calculated and its clinical predictability. The latter, however, appears important to advance NfL rate of change as a biomarker. Future analyses should also assess more accurately the disease period at which NfL rate of change is a better predictor of neurodegeneration and cognitive decline than absolute NfL. Finally, it will be important to translate our findings to sporadic AD and other cerebral proteopathies<sup>13,35</sup>. Studies have indicated that the pathogenesis of familial and sporadic AD are very similar and share similar pathophysiology and progression<sup>36-39</sup>. However, sporadic AD subjects are typically older and have more comorbidities that in turn may influence NfL levels in blood. The latter is however a further argument that absolute NfL levels may be less useful for prediction in early disease stages compared to NfL rate of change.

## **Acknowledgement**

We would like to thank Matthias Staufenbiel and Martin Eichner for support and helpful comments, and Christian Haass and Marc Suarez (Munich) for experimental and logistic support. Data collection and sharing for this project was supported by The Dominantly Inherited Alzheimer's Network (DIAN, UF1AG032438) funded by the National Institute on Aging (NIA) and the German Center for Neurodegenerative Diseases (DZNE). Additional support came from the NIH-funded NINDS Center Core for Brain Imaging (P30NS098577), the National Science Foundation (DGE-1745038), NIH (UL1TR001873 to JMN), the Swiss National Science Foundation (320030-160221 to JK), the National Institute for Health Research University College London Hospitals Biomedical Research Centre and the MRC Dementias Platform UK (MR/L023784/1 and MR/009076/1). We acknowledge the altruism of the participants and their families and contributions of the DIAN research and support staff at each of the participating sites for their contributions to this study.

## **Author Contribution**

All authors were involved in sample and data collection. J.K., O.P., A.A., S.A.K. and C.B. performed the immunoassay work. S.A.S., A.A., G.W., and B.A.G. performed the statistical analysis. M.J., O.P., S.A.S., A.A., and B.A.G. designed the study and wrote the manuscript with the help of the co-authors J.K., S.A.K., C.B., S.G., E.K.-B., C.LaFougere, C.Laske, J.V., J.L., C.L.M., R.M., P.R.S., M.N.R., N.R.G.-R., S.S., B.G., J.M.R., J.M.N., J.C., A.M.G., T.L.S.B., J.C.M., R.J.B., G.W., A.M.F. and E.M.M.

## **Competing Interests**

A.M.G. has consulted for Cognition Therapeutics, Biogen, GSK, Illumina, Eisai, AbbVie and Pfizer and served on the SAB for Denali Therapeutics.

## References

1. Bateman, R.J., *et al.* Clinical and biomarker changes in dominantly inherited Alzheimer's disease. *The New England journal of medicine* **367**, 795-804 (2012).
2. Gordon, B.A., *et al.* Spatial patterns of neuroimaging biomarker change in individuals from families with autosomal dominant Alzheimer's disease: a longitudinal study. *The Lancet. Neurology* **17**, 241-250 (2018).
3. Jack, C.R., Jr., *et al.* NIA-AA Research Framework: Toward a biological definition of Alzheimer's disease. *Alzheimer's & dementia : the journal of the Alzheimer's Association* **14**, 535-562 (2018).
4. Sperling, R.A., Karlawish, J. & Johnson, K.A. Preclinical Alzheimer disease-the challenges ahead. *Nature reviews. Neurology* **9**, 54-58 (2013).
5. Fandos, N., *et al.* Plasma amyloid beta 42/40 ratios as biomarkers for amyloid beta cerebral deposition in cognitively normal individuals. *Alzheimer's & dementia (Amsterdam, Netherlands)* **8**, 179-187 (2017).
6. Mattsson, N., Andreasson, U., Zetterberg, H. & Blennow, K. Association of Plasma Neurofilament Light With Neurodegeneration in Patients With Alzheimer Disease. *JAMA neurology* **74**, 557-566 (2017).
7. Nakamura, A., *et al.* High performance plasma amyloid-beta biomarkers for Alzheimer's disease. *Nature* **554**, 249-254 (2018).
8. Ovod, V., *et al.* Amyloid beta concentrations and stable isotope labeling kinetics of human plasma specific to central nervous system amyloidosis. *Alzheimer's & dementia : the journal of the Alzheimer's Association* **13**, 841-849 (2017).
9. Weston, P.S.J., *et al.* Serum neurofilament light in familial Alzheimer disease: A marker of early neurodegeneration. *Neurology* **89**, 2167-2175 (2017).
10. Mielke, M.M., *et al.* Plasma phospho-tau181 increases with Alzheimer's disease clinical severity and is associated with tau- and amyloid-positron emission tomography. *Alzheimer's & dementia : the journal of the Alzheimer's Association* **14**, 989-997 (2018).
11. Petzold, A. Neurofilament phosphoforms: surrogate markers for axonal injury, degeneration and loss. *Journal of the neurological sciences* **233**, 183-198 (2005).
12. Schlaepfer, W.W. & Lynch, R.G. Immunofluorescence studies of neurofilaments in the rat and human peripheral and central nervous system. *The Journal of cell biology* **74**, 241-250 (1977).
13. Bacioglu, M., *et al.* Neurofilament Light Chain in Blood and CSF as Marker of Disease Progression in Mouse Models and in Neurodegenerative Diseases. *Neuron* **91**, 494-496 (2016).
14. Barro, C., *et al.* Serum neurofilament as a predictor of disease worsening and brain and spinal cord atrophy in multiple sclerosis. *Brain : a journal of neurology* (2018).
15. Brureau, A., *et al.* NF-L in cerebrospinal fluid and serum is a biomarker of neuronal damage in an inducible mouse model of neurodegeneration. *Neurobiology of disease* **104**, 73-84 (2017).
16. Kuhle, J., *et al.* Serum neurofilament light chain in early relapsing remitting MS is increased and correlates with CSF levels and with MRI measures of disease severity. *Multiple sclerosis (Houndmills, Basingstoke, England)* **22**, 1550-1559 (2016).
17. Zhou, W., *et al.* Plasma neurofilament light chain levels in Alzheimer's disease. *Neuroscience letters* **650**, 60-64 (2017).
18. Morris, J.C., *et al.* Developing an international network for Alzheimer research: The Dominantly Inherited Alzheimer Network. *Clinical investigation* **2**, 975-984 (2012).
19. Moulder, K.L., *et al.* Dominantly Inherited Alzheimer Network: facilitating research and clinical trials. *Alzheimer's research & therapy* **5**, 48 (2013).

20. Ryman, D.C., *et al.* Symptom onset in autosomal dominant Alzheimer disease: a systematic review and meta-analysis. *Neurology* **83**, 253-260 (2014).
21. Henriksen, K., *et al.* The future of blood-based biomarkers for Alzheimer's disease. *Alzheimer's & dementia : the journal of the Alzheimer's Association* **10**, 115-131 (2014).
22. McDade, E., *et al.* Longitudinal Cognitive and Biomarker Changes in Dominantly Inherited Alzheimer's Disease. *Neurology* **91**, e1295-e1306 (2018).
23. Sutphen, C.L., *et al.* Longitudinal decreases in multiple cerebrospinal fluid biomarkers of neuronal injury in symptomatic late onset Alzheimer's disease. *Alzheimer's & dementia : the journal of the Alzheimer's Association* **14**, 869-879 (2018).
24. Benzinger, T.L.S., *et al.* Regional variability of imaging biomarkers in autosomal dominant Alzheimer's disease. *Proc. Natl. Acad. Sci. U. S. A.* **110**, E4502-4509 (2013).
25. Burnham, S.C., *et al.* Clinical and cognitive trajectories in cognitively healthy elderly individuals with suspected non-Alzheimer's disease pathophysiology (SNAP) or Alzheimer's disease pathology: a longitudinal study. *The Lancet. Neurology* **15**, 1044-1053 (2016).
26. Jack, C.R., Jr. & Holtzman, D.M. Biomarker modeling of Alzheimer's disease. *Neuron* **80**, 1347-1358 (2013).
27. Lu, C.H., *et al.* Neurofilament light chain: A prognostic biomarker in amyotrophic lateral sclerosis. *Neurology* **84**, 2247-2257 (2015).
28. Rojas, J.C., *et al.* Plasma neurofilament light chain predicts progression in progressive supranuclear palsy. *Annals of clinical and translational neurology* **3**, 216-225 (2016).
29. Norgren, N., Karlsson, J.E., Rosengren, L. & Stigbrand, T. Monoclonal antibodies selective for low molecular weight neurofilaments. *Hybridoma and hybridomics* **21**, 53-59 (2002).
30. Byrne, L.M., *et al.* Neurofilament light protein in blood as a potential biomarker of neurodegeneration in Huntington's disease: a retrospective cohort analysis. *The Lancet. Neurology* **16**, 601-609 (2017).
31. Karran, E., Mercken, M. & De Strooper, B. The amyloid cascade hypothesis for Alzheimer's disease: an appraisal for the development of therapeutics. *Nature reviews. Drug discovery* **10**, 698-712 (2011).
32. Fagan, A.M., *et al.* Longitudinal change in CSF biomarkers in autosomal-dominant Alzheimer's disease. *Science translational medicine* **6**, 226ra230 (2014).
33. Kinnunen, K.M., *et al.* Presymptomatic atrophy in autosomal dominant Alzheimer's disease: A serial magnetic resonance imaging study. *Alzheimer's & dementia : the journal of the Alzheimer's Association* **14**, 43-53 (2018).
34. Shahim, P., *et al.* Serum neurofilament light protein predicts clinical outcome in traumatic brain injury. *Scientific reports* **6**, 36791 (2016).
35. Jucker, M., & Walker, L.C. Propagation and spread of pathogenic protein assemblies in neurodegenerative diseases. *Nature Neuroscience* **21**, 1341-1349 (2018).
36. Bateman, R.J., *et al.* Autosomal-dominant Alzheimer's disease: a review and proposal for the prevention of Alzheimer's disease. *Alzheimer's research & therapy* **3**, 1 (2011).
37. Cairns, N.J., *et al.* Neuropathologic assessment of participants in two multi-center longitudinal observational studies: the Alzheimer Disease Neuroimaging Initiative (ADNI) and the Dominantly Inherited Alzheimer Network (DIAN). *Neuropathology : official journal of the Japanese Society of Neuropathology* **35**, 390-400 (2015).
38. Tang, M., *et al.* Neurological manifestations of autosomal dominant familial Alzheimer's disease: a comparison of the published literature with the Dominantly Inherited Alzheimer Network observational study (DIAN-OBS). *The Lancet. Neurology* **15**, 1317-1325 (2016).



39. Thomas, J.B., *et al.* Functional connectivity in autosomal dominant and late-onset Alzheimer disease. *JAMA neurology* **71**, 1111-1122 (2014).

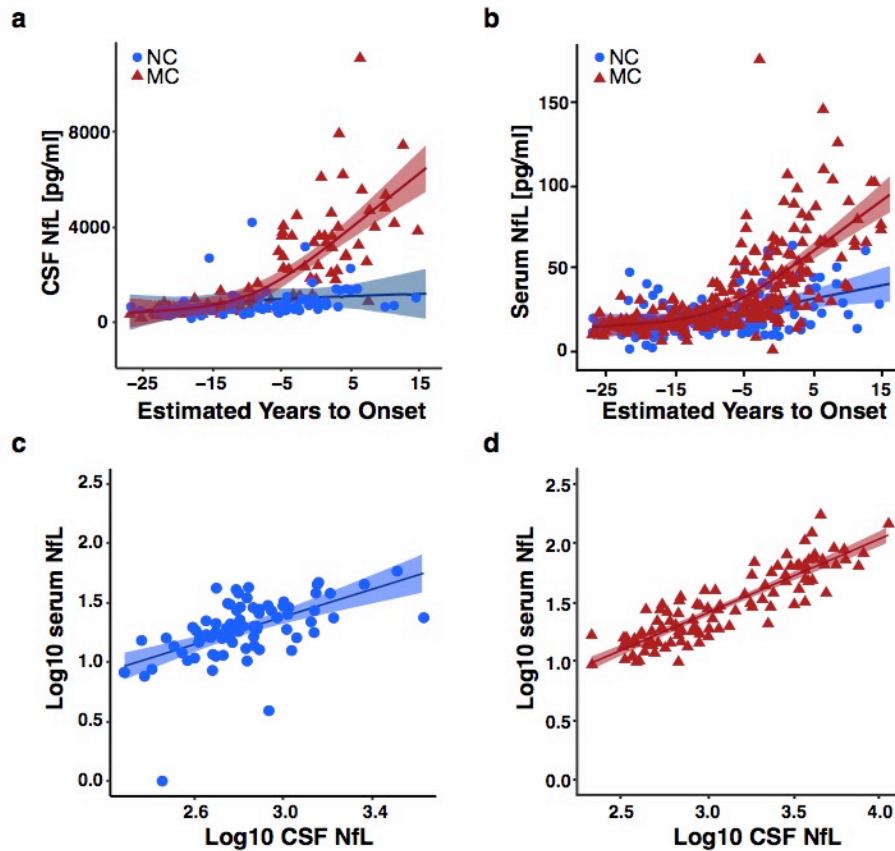


**Figure 1.** CSF and serum NfL levels are highly correlated and divert between mutation carriers (MC) and non-carriers (NC) already in the presymptomatic phase. **(a)** CSF NfL values of NC (blue, n=80), MC (red, n=107) as a function of EYO. Shown is -27 until +15 years before or after EYO, respectively. **(b)** Serum NfL for NC (n=162), and MC (n=243) as a function of EYO. For (a) and (b) the shaded areas represent 99% credible intervals around the model estimates. The curves and credible intervals are drawn from the actual distributions of model fits derived by the Hamilton Markov chain Monte Carlo analyses (see Methods). The first EYO where NC and MC differed was determined to be the first point where the 99% credible intervals around the differences distribution between NC and MC did not overlap 0. (-6.8 years before EYO for both CSF and serum, see Extended Data Fig. 1). It should be noted, that our analysis is influenced by the available number of participants. Thus, results do not represent absolute measures, but rather relative EYO points where we can detect effects given the limitations of sample size. **(c, d)** Significant associations from linear mixed effect models between CSF NfL and serum NfL in NC (n=80; B[SE]=0.350 [.14],  $p=0.014$ ) and MC (n=107; B[SE]=0.612[.05],  $p<2.0e-16$ ) were found.

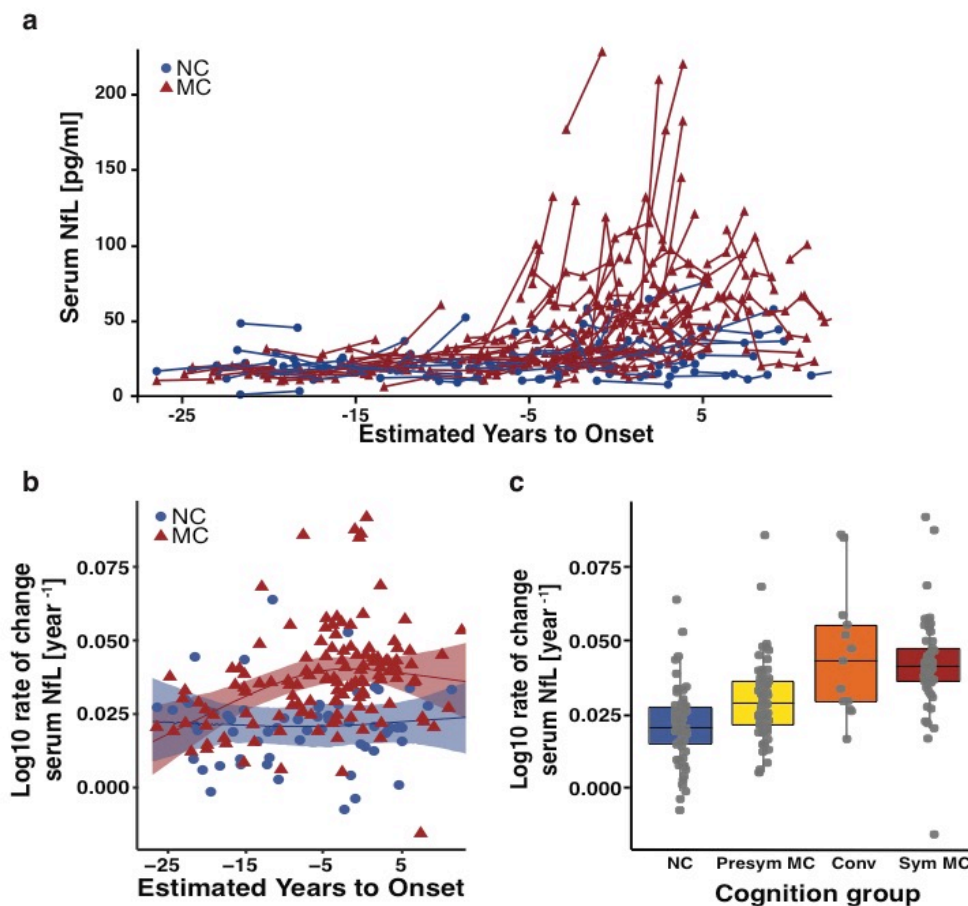


**Figure 2.** Longitudinal serum NfL distinguishes mutation carriers (MC) from non-carriers (NC) very early in the presymptomatic disease process, with NfL rate of change peaking in individuals converting from the presymptomatic to the symptomatic phase. **(a)** Spaghetti plot showing longitudinal serum NfL for NC (blue,  $n=63$ ) and MC (red,  $n=133$ ) as a function of EYO. The displayed x-axis range is limited to -27.5 until +12.5 years before or after EYO, respectively, in order to maintain blinding of some individuals contributing to this dataset. In addition, again to maintain blinding the EYO of two participants (one MC and one NC) was set to the mean of both EYO values. A logarithmic version of the spaghetti plot is shown in Extended Data Fig. 3a to better appreciate that changes between MC and NC already occur at presymptomatic levels. **(b)** Estimated rate of change per year in serum NfL (see Method for calculation) plotted against baseline EYO for MC and NC (shown is -27.5 until +12.5). Individual random-effect slope estimates are plotted as colored symbols. The shaded areas represent 99% credible intervals around the model estimates. The curves and credible intervals are drawn from the actual distributions of model fits derived by the Hamilton Markov chain Monte Carlo analyses. The first EYO where groups (NC and MC) differed was determined to be the first point where the 99% credible intervals around the differences distribution between NC and MC did not overlap 0 (-16.2 years before EYO; see Extended Data Fig. 3b). An even earlier deviation of the two curves was calculated when linear regression analyses were performed (Extended Data Fig. 3c). **(c)** Rate of change per year in serum NfL across four groups differing by mutation and cognitive status: NC (blue,  $n=63$ );

presymptomatic MC (yellow, n=65) are individuals who scored as CDR=0 across all visits; Converters (orange, n=13) are MC who scored as CDR=0 at baseline and CDR>0 at subsequent visits; Symptomatic MC (red, n=55) are individuals who scored as CDR>0 across all visits. The boxes map to the median, twenty-fifth and seventy-fifth quintiles, and whiskers extend to the 1.5x interquartile range (IQR). Comparisons were done with linear mixed effect models. Presymptomatic MC had significantly higher annual rate of change compared to NC (B[SE]=.009[.003],  $p=6.71e-04$ ). Converters had significantly higher rate of change compared to both NC (B[SE]=.024[.004]  $p=3.05e-07$ ) and presymptomatic MC (B[SE]=.015[.005],  $p=1.19e-03$ ). Symptomatic MC had significantly higher rates of change compared to both NC (B[SE]=.020[.003],  $p=8.78e-12$ ) and presymptomatic MC (B[SE]=.011[.003],  $p=1.51e-04$ ). There was no difference between converters and symptomatic MC (B[SE]=-.004[.005],  $p=0.445$ ).

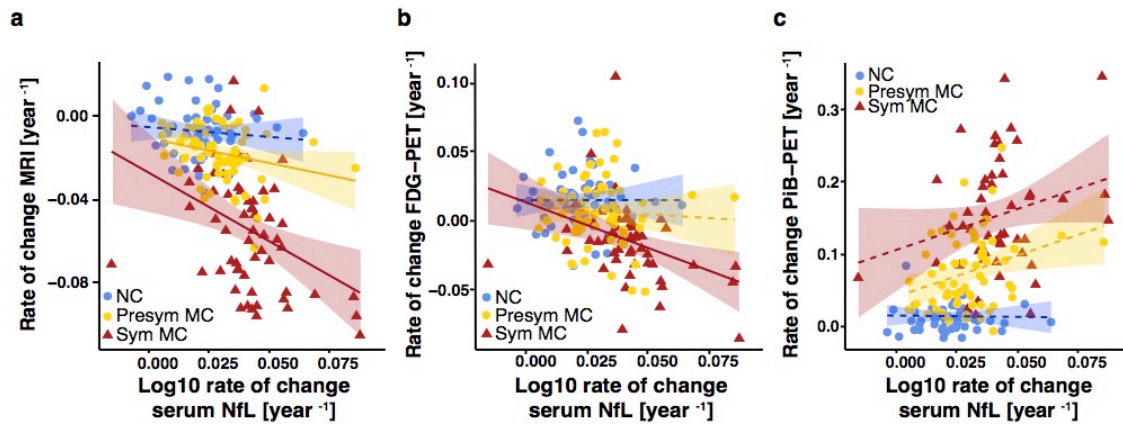


**Figure 3.** Rate of change per year in serum NfL in mutation carriers mirrors rate of change in cortical thinning. **(a)** Relationship between estimated annual rate of change in serum NfL and estimated annual rate of change in precuneus cortical thickness for non-carriers (NC), presymptomatic mutation carriers (Presym MC) and symptomatic MC (Sym MC; including converters to the symptomatic phase, see Figure 2c). Results from linear mixed effect models revealed a significant association in symptomatic MC ( $n=60$ ) ( $B[SE]=-0.914[0.367]$ ,  $p=0.018$ ) and a close to significant association in presymptomatic MC ( $n=65$ ) ( $B[SE]=-0.325[0.166]$ ,  $p=0.054$ ), but not in NC ( $n=59$ ) ( $B[SE]=-0.210[0.149]$ ,  $p=0.886$ ). Between group comparison indicated that rate of change in serum NfL was slightly more associated in symptomatic MC compared to asymptomatic MC ( $B[SE]=-0.573[0.305]$ ,  $p=0.063$ ). **(b)** Relationship between rate of change in serum NfL and rate of change in precuneus FDG-PET. Using linear mixed effect models, a positive association was only found in symptomatic MC ( $n=55$ ) ( $B[SE]=-1.149[0.501]$ ,  $p=0.031$ ) but not in presymptomatic MC ( $n=64$ ) ( $B[SE]=-0.227[0.456]$ ,  $p=0.620$ ) or NC ( $n=55$ ) ( $B[SE]=0.161[0.347]$ ,  $p=0.465$ ). **(c)** Relationship between rate of change in serum NfL and rate of change in in precuneus A $\beta$ -PET. Using linear mixed effect models, no significant association in any of the three groups were found, NC ( $n=57$ ) ( $B[SE]=-0.468[0.547]$ ,  $p=0.403$ ); presymptomatic MC ( $n=64$ ) ( $B[SE]=1.248[1.000]$ ,  $p=0.216$ ); symptomatic sMC ( $n=51$ ) ( $B[SE]=1.805[1.556]$ ,  $p=0.266$ ). The shaded area around each linear fit line represents 1 standard error. Note that not all participants with longitudinal NfL measurements had imaging parameters available and thus the n's are slightly lower compared to those in Fig. 2c.

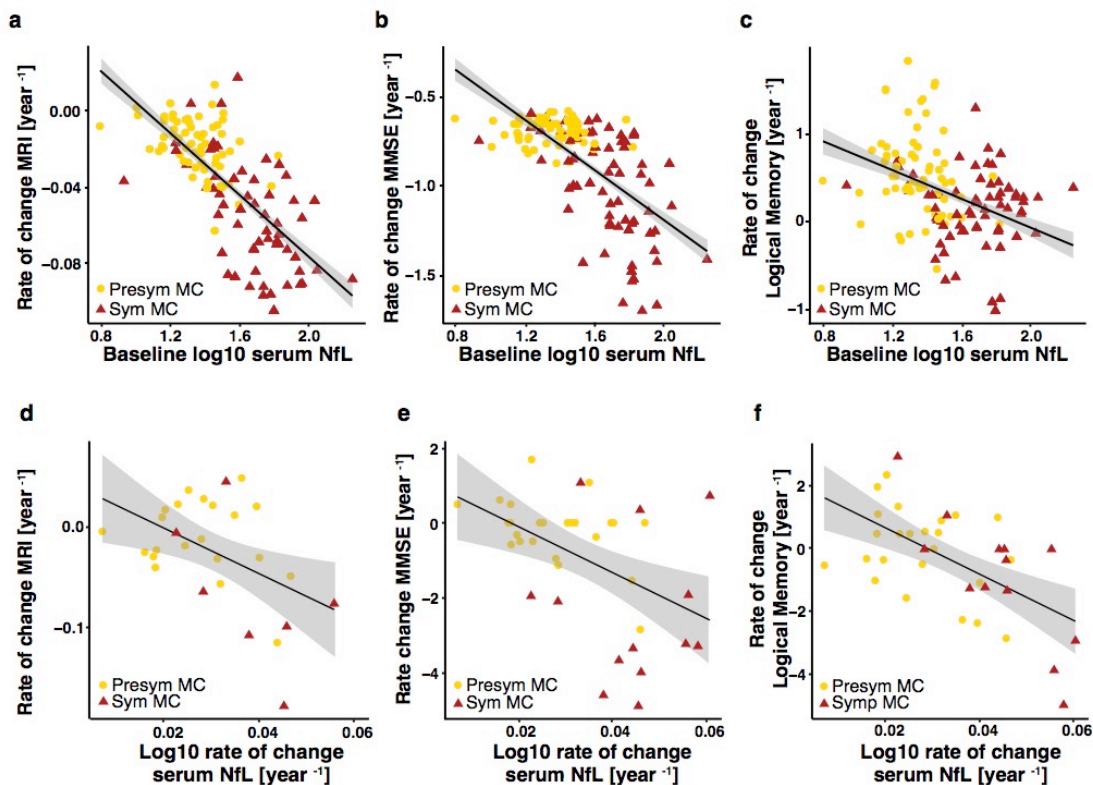
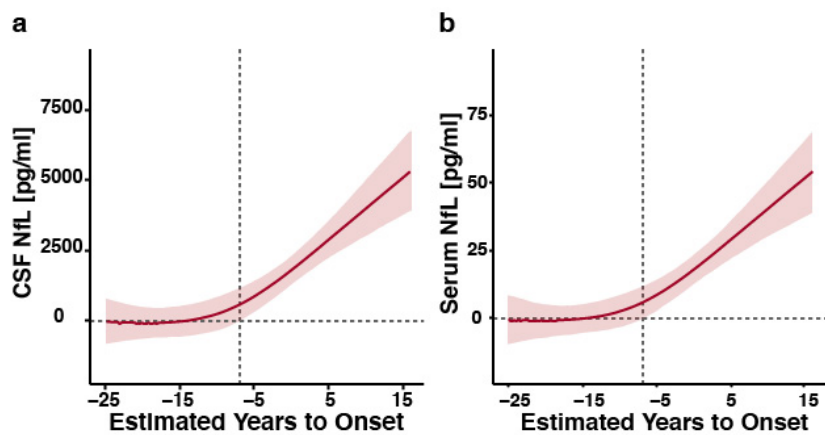
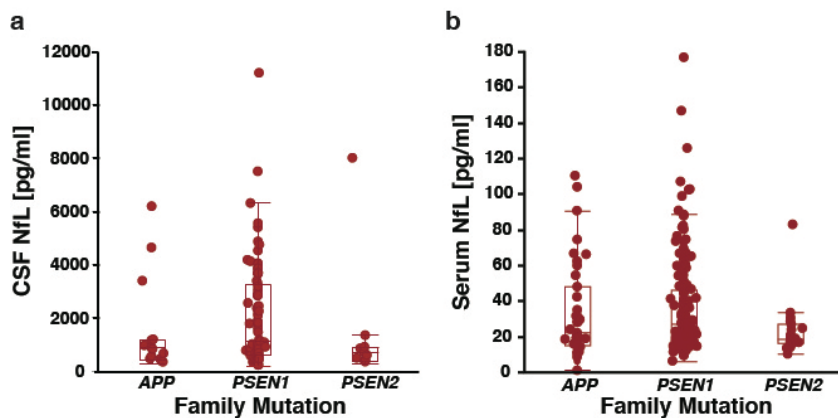


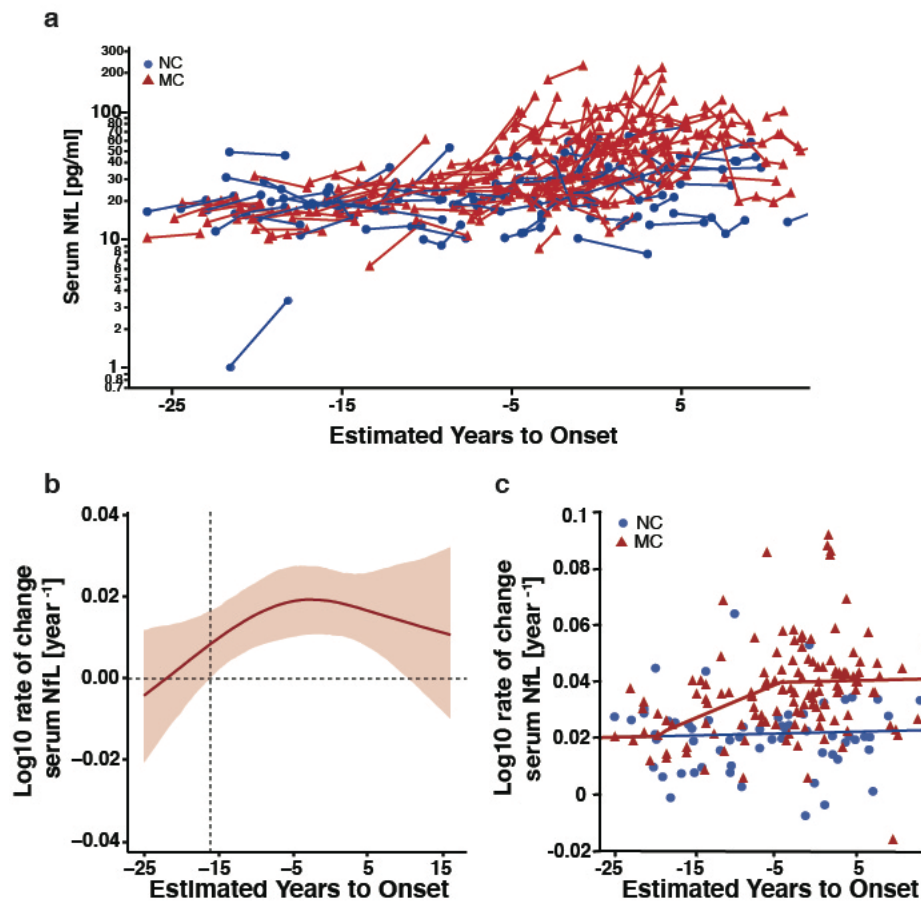
**Figure 4.** Prediction of changes in cortical thinning and cognition by baseline serum NfL (retrospective prediction) and serum NfL rate of change (prospective prediction). **(a-c)** Higher baseline serum NfL levels were significantly associated with an increased rate of change in (a) cortical thickness ( $n=125$ ;  $B[SE]=-0.105[0.013]$ ,  $p=4.47e-13$ ), (b) MMSE ( $n=132$ ;  $B[SE]=-3.980[0.537]$ ,  $p=2.38e-11$ ), and (c) Logical Memory Test (immediate recall,  $n=133$ ;  $B[SE]=-1.478[0.502]$ ,  $p=0.004$ ). A similar significance ( $p=0.015$ ) was obtained for the Logical Memory Test delayed recall. Linear mixed effect models (see methods) were run with all MC together ( $n=125$ ) because of the high degree of overlap in cognitive and biomarker levels between presymptomatic and symptomatic MC. However, at least for cortical thickness separate analyses for presymptomatic and symptomatic MC were also significant ( $n=65$ ; presymptomatic MC, yellow;  $B(SE)=-0.03(0.01)$ ,  $p=0.047$  and  $n=60$ ; symptomatic MC, red;  $B(SE)=-0.10(0.03)$ ,  $p=0.002$ , respectively). **(d-f)** In a true prospective design MC returning for follow-up visits after the last serum collection were included in the analysis. Individual's rate of change in serum NfL levels predicted subsequent cortical thinning (d;  $n=30$ ;  $B[SE]=-1.867[0.769]$ ,  $p=0.024$ ). The same predictive associations were also significant for MMSE (e;  $n=37$ ;  $B[SE]=-52.23[20.19]$ ,  $p=0.015$ ) and Logical Memory Test scores (f; immediate recall,  $n=37$ ;  $B[SE]=-75.91[18.07]$ ,  $p=0.0002$ ). Presymptomatic and symptomatic MC are plotted in different colors (yellow and red, respectively) for descriptive purposes (see above). Note that not all participants with baseline NfL measurements had longitudinal MRI imaging and longitudinal cognitive parameters available and thus the  $n$ 's in (a-c) are slightly lower compared to those in Supplementary Table 2. This was also true for the MC returning for follow-up visits after the last serum collection (d-f). The shaded area around each linear fit line represents 1 standard error from linear mixed effect models.



**Extended Data Figure 1.** Difference distribution curve for baseline (cross-sectional) CSF and serum NfL levels in mutation carriers (MC) and non-carriers (NC). (a) Difference of posterior distribution for baseline CSF NfL (n=187) and (b) baseline serum NfL (n=405) as a function of EYO. Solid red lines depict median of difference distribution, and shaded area represents 99% equal-tailed credible intervals. EYO was considered statistically significant if the 99% equal-tailed credible intervals of the posterior distribution did not overlap zero (6.8 years before EYO for both baseline CSF and serum NfL). For absolute values of baseline CSF and serum NfL see Fig. 1a and b.

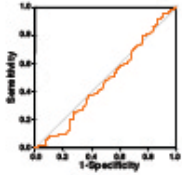
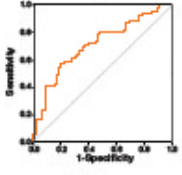
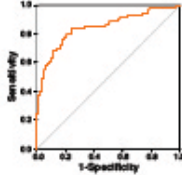
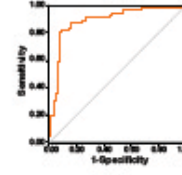


**Extended Data Figure 2.** No difference in baseline CSF and serum NfL levels among APP, PSEN1 and PSEN2 mutation carriers. (a) Pairwise t-test comparisons of CSF NfL levels of carriers of a mutation in APP (n=14), PSEN1 (n=82), or PSEN2 (n=11). (b) Same analysis, using pairwise t-test for serum NfL of carriers of a mutation in APP (n=39), PSEN1 (n=185), or PSEN2 (n=19). No differences in log CSF or log serum NfL were found between the groups ( $F(2;104)=1.8108$ ,  $p=0.1686$  and  $F(2;240)=1.9205$ ,  $p=0.1488$ , respectively). Similarly, no differences were found by pairwise t-test when age and disease state (presymptomatic, symptomatic) were treated as covariates. The boxes map to the median, twenty-fifth and seventy-fifth quintiles, and whiskers extend to the 1.5xIQR.

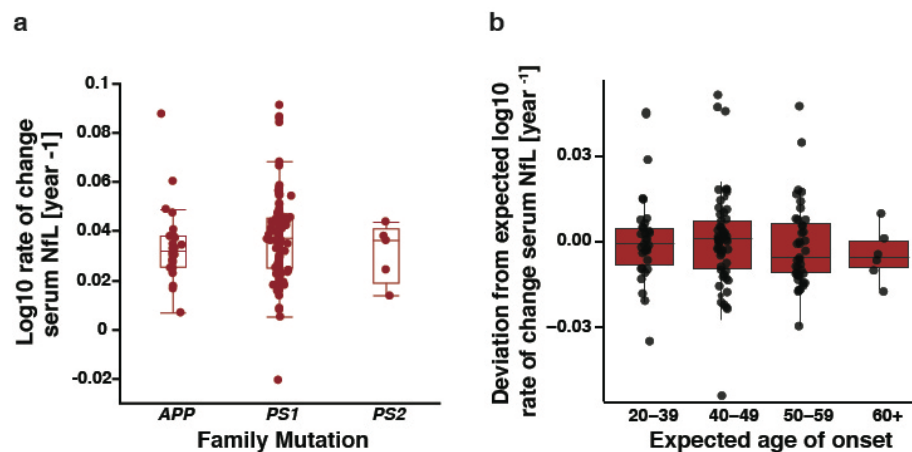


**Extended Data Figure 3.** Longitudinal serum NfL and bifurcation of mutation carriers (MC) from non-carriers (NC). **(a)** Spaghetti plot showing longitudinal serum NfL for NC ( $n=63$ , blue) and MC ( $n=133$ , red) as a function of EYO. These are the same data as in Fig. 2a but with a logarithmic scale on Y-axis to better appreciate the changes during the presymptomatic stage (for details see Fig. 2a). **(b)** Difference of posterior distribution for serum NfL rate of change between MC and NC, as a function of EYO ( $n=196$ ). Solid red line depicts median of difference distribution, and shaded area represents 99% equal-tailed credible intervals. EYO was considered statistically significant if the 99% equal-tailed credible intervals of the posterior distribution did not overlap zero (16.2 years before EYO). **(c)** Individual estimated rate of change in serum NfL (same data as in Fig. 2b,  $n=63$  for NC and  $n=133$  for MC). Here a regression analysis was performed with two breaks of slope (see Method for calculation). With this model the first bifurcation point was found at -18.6 years before EYO, the second at -5.8 years before EYO.



|                      | NC vs. presymptomatic MC  |   | NC vs. symptomatic MC  |   |
|----------------------|---|---|--|---|
|                      | Cross-sectional<br>(Baseline value)   | Longitudinal<br>(Rate of change per year)   | Cross-sectional<br>(Baseline value)  | Longitudinal<br>(Rate of change per year)   |
| ROC curve            |  |  |  |  |
| AUC                  | 0.49  | 0.70  | 0.85   | 0.89  |
| Specificity          | 14%   | 78%   | 75%  | 89%   |
| Sensitivity          | 92%   | 58%   | 85%  | 82%   |
| Cutoff value         | 37.4 pg/ml  | 0.027   | 27.9 pg/ml   | 0.033   |
| n                    | Total=319<br>(NC=162, preMC=157)  | Total=141<br>(NC=63, preMC=78)  | Total=248<br>(NC=162, sMC=86)  | Total=118<br>(NC=63, sMC=55)  |
| p-value ( $\chi^2$ ) | 0.6485  | 0.0002  | <0.0001  | <0.0001   |

**Extended Data Figure 4.** Rate of change per year of serum NfL is a better parameter to distinguish presymptomatic and symptomatic mutation carriers (MC) from non-carriers (NC) compared to single cross-sectional serum NfL. Receiver operating characteristic (ROC) analysis for NC vs presymptomatic MC and NC vs symptomatic MC with cross-sectional (baseline serum NfL) and longitudinal (serum NfL rate of change per year) data. True-positive fraction (sensitivity) is on the Y-axis and false-positive fraction (1-specificity) on the X-axis. The area under the curve (AUC, accuracy), as well as cutoff value and  $\chi^2$  p-value from logistic regression are shown. The chance level of AUC is 0.50. Converters (for rate of change; see Fig. 2c) were considered presymptomatic MC.



**Extended Data Figure 5.** No difference in serum NfL rate of change among APP, PSEN1 and PSEN2 mutation carriers and no association with estimated age of onset. **(a)** Using pairwise t-tests, no differences in rate of change log serum NfL [year<sup>-1</sup>] levels among APP (n=24), PSEN1 (n=104) and PSEN2 (n=5) mutation carriers ( $F(2;130)=0.4678$ ,  $p=0.6274$ ) was found. Similarly, no differences were found when age and disease state (presymptomatic, symptomatic) were treated as covariates in a pairwise t-test. **(b)** No difference between an individual's deviation from the EYO-adjusted median rate of change in NfL and their expected age of symptom onset (AO) using linear mixed effect models. Individuals were grouped in 4 categories with expected symptom onset at 20-39 (n=17), 40-49 (n=54), 50-59 (n=56), and over 60 years of age (n=6); (group comparisons,  $p$ 's>0.146). See methods for calculations. The boxes map to the median, twenty-fifth and seventy-fifth quintiles, and whiskers extend to the 1.5xIQR.

## Methods

### Participants

Participants at 50% risk of carrying an autosomal-dominant AD mutation in one of three genes (*APP*, *PSEN1*, *PSEN2*) were enrolled in the Dominantly Inherited Alzheimer Network Observational study (DIAN, NIA U19 AG032438) ([dian.wustl.edu](http://dian.wustl.edu); [clinicaltrials.gov NCT00869817](https://clinicaltrials.gov/NCT00869817))<sup>18</sup>. DIAN participants are assessed at baseline and subsequent follow-up visits (annually to every third year). Assessment included collection of body fluids (CSF, blood), clinical testing (Clinical Dementia Rating, CDR), neuropsychological testing (including Mini-Mental State Examination, MMSE, raw scores; and Logical Memory subtest of the Wechsler Memory Scale–Revised [WMS-R, story A], raw scores for immediate and delayed recall), and imaging modalities (MRI, PET with Pittsburgh Compound B [PiB], and <sup>18</sup>F-Fluorodeoxyglucose [FDG]) as described in earlier publications<sup>1,2,40-42</sup>. The institutional review board at Washington University in St. Louis provided supervisory review and human studies approval. Participants or their caregivers provided informed consent in accordance with their local institutional review boards. NfL analysis in the DIAN cohort was approved by the ethics-committee at the medical faculty of the University of Tübingen, Germany (718/2014B02). The detailed number of participants (mutation carriers, MC; non-carriers, NC) for baseline and longitudinal measurements are given in Supplementary Table 1 and 2 and legends of Fig. 2-4.

### Clinical assessment and expected years of symptom onset

The presence of dementia (symptoms) was assessed using CDR<sup>41</sup>. Clinical evaluators were blinded to the participant's mutation status. For every visit a participant's estimated years from expected symptom onset (EYO) was calculated based upon the participant's age at the visit relative to their "mutation-specific" expected age at dementia onset. The "mutation-specific" expected age of dementia onset was computed by averaging the reported age of dementia onset across individuals with the same specific mutation<sup>20</sup>. If the "mutation-specific" expected age at dementia onset was unknown, EYO was calculated from the age at which parental cognitive decline began. The parental age of clinical symptom onset was determined by a semi-structured interview with the use of all available historical data. EYO was calculated identically for both mutation carriers and non-carriers. Mutation status was determined using PCR-based amplification of the appropriate exon followed by Sanger sequencing<sup>1</sup>.

### NfL measurements in CSF and blood

Fluids were collected in the morning under fasting conditions by venipuncture using 21G butterfly and Red top plain vacutainer tubes (Becton Dickinson, Oakville, ON, Canada). After blood collection the tubes were left upside at room temperature for 30 minutes to allow clotting. After clotting tubes were centrifuged at 2,000 g for 15 min at room temperature. Serum was taken with a disposable non-sterile transfer pipette into a single transfer tube (#60.541, Sarstedt AG&CO.KG, Nümbrecht, Germany) and immediately frozen on dry ice. After venipuncture, CSF was collected (by gravity drip into two 13 ml polypropylene tubes) via standard lumbar puncture procedures (L4/L5) using an atraumatic Sprotte spinal needle (22Ga). As with serum, CSF was flash-frozen upright on dry ice. Samples collected in the US were shipped overnight on dry ice to the DIAN biomarker core laboratory at Washington University, St. Louis, MO, USA, whereas samples collected at non-US sites were stored at -80°C and shipped quarterly on dry ice to St. Louis. At the core laboratory the frozen samples were subsequently thawed, combined into a single polypropylene tube of serum or CSF and

aliquoted (300 or 500  $\mu$ l) into polypropylene microcentrifuge tubes (#05-538-69C, Corning Life Science, Corning, NY, USA), after which they were re-flash frozen on dry-ice and stored at  $-80^{\circ}\text{C}$ . For the current study, all available DIAN serum samples (data freeze 11) were shipped to the DIAN Tübingen. CSF samples (data freeze 9) were shipped to the DIAN Munich site first and used for another analysis before shipping them to the DIAN Tübingen site. Thus, the CSF sample had one additional freeze-thawing cycle in Munich, however prior work has indicated no significant effect of up to 4 freeze-thawing cycles on NfL in CSF<sup>43</sup>.

CSF and serum NFL measurements were performed using a highly sensitive Single Molecule Array (SIMOA) assay using the capture monoclonal antibody (mAB) 47:3 and the biotinylated detector antibody mAB 2:1 (Uman Diagnostics, Umeå, Sweden)<sup>44</sup>. The samples were measured in duplicate on a Simoa HD-1 platform (Quanterix) using a 2-step neat assay. Serum samples were measured at 1:4 and CSF at 1:10 dilution (tris base saline (TBS), 0.1% Tween 20, 1% nonfat milk powder, Heteroblock (300  $\mu\text{g/ml}$ , Omega Biologicals, Bozeman, MT, USA)). Batch prepared calibrators (bovine lyophilized NfL) ranging from 0 to 10,000  $\text{pg/ml}$  were stored at  $-80^{\circ}\text{C}$  (Uman Diagnostics). All samples were measured blinded. For serum, the mean intra-assay coefficient of variation (CV) of duplicate determinations for concentration was 4.2%. In CSF, the mean intra-assay CV was 3.7%. Inter-assay variability was evaluated with 3 native serum samples and 3 native CSF samples. Inter-assay CVs for serum were 7.7% (mean concentration 13.3  $\text{pg/ml}$ ), 2.9% (30.9  $\text{pg/ml}$ ), and 3.7% (269.9  $\text{pg/ml}$ ). In CSF, inter-assay CVs were 2.4% (445.4  $\text{pg/ml}$ ), 12.2% (1486.3  $\text{pg/ml}$ ), and 13.3% (14049.0  $\text{pg/ml}$ ). Note that the concentrations ( $\text{pg/ml}$ ) are calculated from the full-length NfL calibrator and thus may overestimate the concentration of an NfL fragment in blood.

## Imaging

Magnetic resonance imaging (MRI) was performed at the different DIAN sites on 3T scanners using the Alzheimer's Disease Neuroimaging Initiative (ADNI) protocol. T1-weighted images (1.1 $\times$ 1.1 $\times$ 1.2 mm voxels) were acquired for all participants. The ADNI Imaging Core screened images for artifacts and protocol compliance. FreeSurfer 5.3 was used to perform volumetric segmentation and cortical surface reconstruction to define subcortical and cortical regions of interest (ROIs). Members of the DIAN imaging core examined each segmentation and edited as needed. Cortical thickness measures were averaged across hemispheres. As the precuneus region has been shown to be most sensitive to AD pathophysiology in autosomal-dominant AD<sup>2,24</sup>, we *a priori* focused our analyses on this region.

$\text{A}\beta$ -PET- imaging was done using a bolus injection of  $^{11}\text{C}$ -PiB. Acquisition consisted of a 70-min scan starting at injection or a 30-min scan beginning 40 min after injection. Data in the common 40–70 min timeframe was converted to regional standardized uptake value ratios (SUVRs) relative to the cerebellar grey matter using FreeSurfer derived regions of interests (ROIs) (PET Unified Pipeline, <https://github.com/ysu001/PUP>). Metabolic imaging was done with FDG-PET with a 30 min dynamic acquisition beginning 30 min after injection. Data from the 40-60 min timeframe were converted to SUVRs relative to cerebellar grey matter. The ADNI PET Core verified that PET images were acquired using the established protocol and free of substantial artifacts. All PET data were partial volume corrected using a regional spread function technique. Scanner-specific spatial filters were applied to achieve a common resolution (8 mm) across PET scanners. MRI and PET data acquisition and processing has been described in detail in previous studies<sup>1,2,24</sup>. Again, for the present analyses, we averaged SUVR values from the bilateral precuneus ROIs defined on the MRI.

## Statistical analysis

*Relating baseline CSF and serum NfL*

The relationship between baseline CSF and serum NfL was determined by using linear mixed-effects (LME) models implemented in R Version 3.4.2 and RStudio Version 1.1.453 using lme4, including a random intercepts term for family and fixed effect for baseline age, sex, and baseline CSF NfL, with baseline serum NfL as the dependent variable. Separate models were fit for NC and MC. Baseline CSF and serum NfL values were log-transformed (due to non-normal distribution) before being entered into the model. See also Supplementary statistical analysis.

#### *Baseline CSF and serum NfL as a function of EYO*

The relationship between EYO and baseline CSF and serum NfL values were estimated using LMEs. As previously done, to account for potential non-linear effects, EYO was modeled as a restricted cubic spline with knots at the 0.10, 0.50, and 0.90 quantiles<sup>2</sup>. The LME models for baseline NfL values (CSF or serum) included fixed effects for mutation status, the linear EYO component, the cubic EYO component, the linear EYO by mutation status interaction, the cubic EYO by mutation status interaction, and a random intercept for family. Model parameters were estimated using an open source package for Hamilton Markov chain Monte Carlo analyses, STAN (<http://mc-stan.org/>)<sup>45,46</sup>, implemented using R. This resampling approach leads to a distribution of parameters estimates across iterations. From this distribution it is possible to estimate the 99% credible intervals of the model fits at every EYO for NC, MC, and the distribution of the difference between NC and MC. The first EYO where groups (NC and MC) differed was determined to be the first point where the 99% credible intervals around the differences distribution between NC and MC did not overlap 0. See also Supplementary statistical analysis.

#### *Calculating the rate of change in biomarkers*

Longitudinal data was modeled using LMEs. LMEs are a powerful approach to account for the covariance structure introduced by serial measurements and are ideal to deal with imperfect timing or unbalanced number of data points. The rate of change in log-transformed serum NfL for each individual was modeled using an LME with fixed effects of time from baseline (in years), mutation status, and a time from baseline by mutation status interaction, and a random intercept for family, as well as random slope and intercept terms for each participant. The rate of NfL change for each individual was extracted from the model estimates for subsequent analyses. This model was also used for generating rate of change for cortical thickness, FDG-PET, and PiB-PET, for each individual (for plotting purposes). See also Supplementary statistical analysis.

#### *Longitudinal serum NfL as a function of EYO and cognitive status*

As with the cross-sectional estimates, the relationship between EYO and rate of change in serum NfL was estimated using an LME in STAN. EYO was modeled as a restricted cubic spline with knots at the 0.10, 0.50, and 0.90. The LME model for rate of change in serum NfL included fixed effects for mutation status, the linear EYO component, the cubic EYO component, the linear EYO by mutation status interaction, the cubic EYO by mutation status interaction, and a random intercept for family. Model parameters were estimated using an open source package for Hamilton Markov chain Monte Carlo analyses, STAN, implemented using R. Again, this resampling approach leads to a distribution of parameters estimates across iterations, resulting in 99% credible intervals of the model fits at every EYO for NC, MC, and the distribution of the difference between NC and MC. The first EYO where groups (NC and MC) differed was determined to be the first point where the 99% credible intervals around the differences distribution between NC and MC did not overlap 0.

To determine whether the extracted rate of change in serum NfL was significantly different across mutation status and cognitive status we categorized MC based on cognitive status where presymptomatic MC were individuals who scored as CDR=0 across all visits (n=65), Converters were MC who scored as CDR=0 at baseline and CDR>0 at subsequent visits (n=13), and symptomatic MC were individuals who scored as CDR>0 across all visits (n=55). We used LME models, including a random intercept for family and fixed effects for baseline age, sex, and Group (i.e., NC, presymptomatic MC, converter, or symptomatic MC), where Group was the term of interest, and the extracted rate of change in serum NfL as the dependent variable. Models were computed using lme4 in R. See also Supplementary statistical analysis.

#### *Association between expected age of onset and deviation from the EYO-adjusted median rate of change in NfL*

The hypothesis was tested if individuals who have an earlier expected age of onset (AO; e.g., AO of 30 years old vs 55 years old) have an accelerated NfL rate of change. First, to determine if a participant deviated from its expected NfL rate of change, given its baseline EYO, we calculated the median rate of change in NfL at each EYO, generated from model estimates (for calculation see “Baseline CSF and serum NfL and longitudinal NfL as a function of EYO” in the Supplementary statistical analysis; for depiction of median value see red line in Fig. 2b). We then took each participant's extracted NfL rate of change and subtracted the median value corresponding to its baseline EYO. This resulting value represented the deviation from the expected value, whereby a positive value on this deviation measure indicates that an individual has a higher rate of change in serum NfL (i.e., worse) than would be expected given their EYO. Conversely, a negative value on this deviation measure indicates that an individual has a lower rate of change in serum NfL (i.e., better) than would be expected given their EYO. Next, in order to investigate if there was a relationship between individuals with the higher deviation measure and earlier expected AO, we grouped individuals by their expected AO (determined by their specific mutation type, grouped AO 20-39, 40-49, 50-59, and 60+). See also Supplementary statistical analysis.

#### *Relating NfL rate of change with imaging rate of change*

The longitudinal relationship between the rate of change in serum NfL and concurrent rate of change in cortical thickness, metabolism, or A $\beta$  accumulation was determined within each group of interest (i.e. NC, presymptomatic MC, and symptomatic MC). Therefore, separate models were run for each NC, presymptomatic MC, and symptomatic MC groups. The dependent term for each model was an imaging biomarker with fixed effect terms for baseline age, sex, time from baseline, extracted rate of change in serum NfL, and the interaction between time from baseline and the rate of change in serum NfL. Models contained random slope and intercept terms for participants and random intercepts for family. The primary term of interest was the interaction between the rate of change in serum NfL and the time from baseline term. Models were fit using lme4 in R.

To determine whether the relationship between groups was different, a model, for each imaging modality, containing all groups was run. Each model was fit containing fixed effect terms for baseline age, sex, time from baseline, extracted rate of change in serum NfL, group (NC, presymptomatic MC, or symptomatic MC), and two and three-way interaction between time from baseline, rate of change in serum NfL, and group. Converters were included as part of the symptomatic MC group. The models also included random slope and intercept terms for the participants and random intercepts for family. The dependent variables were the

longitudinal measures for cortical thickness, glucose metabolism, or A $\beta$  deposition in the precuneus ROI. See also Supplementary statistical analysis.

#### *Serum NfL at baseline predicting of the annual changes in cortical thickness and cognition*

To examine whether baseline serum NfL could predict subsequent change in cortical thickness and cognition in MC we fit LME models with random slope and intercept terms for participants, random intercepts for family, and fixed effect terms for baseline age, sex, time, log-transformed baseline serum NfL, and an interaction between time and baseline serum NfL. The interaction term was the term of interest. The dependent terms entered into the models were longitudinal precuneus cortical thickness measurements, MMSE scores, and Logical Memory Test scores. If significant, an association of baseline serum NfL with rate of change in cortical thickness or cognition was assumed. See also Supplementary statistical analysis.

#### *Prospective prediction of cortical thickness and cognition by serum NfL rate of change*

To determine whether the rate of change in serum NfL could predict subsequent change in cortical thickness or cognition, we conducted a truly prospective study, whereby after longitudinal serum collection for NfL, we collected additional imaging and neuropsychological data on 39 MC. There were 28 individuals who completed additional imaging and neuropsychological testing, 9 who completed only additional neuropsychological testing but no MRI, and 2 who completed an additional MRI but not neuropsychological testing. To determine the rate of change in cortical thickness and cognition (MMSE, Logical Memory) between the imaging and cognitive assessment concurrent to the participant's last blood draw and follow-up session, we fit an LME for each participant, where the dependent variable was the imaging or cognitive variables of interest at last serum visit and follow-up visit and the independent variable was time between visits. Models were run in R. We then used this rate of change for cortical thickness or cognition as the dependent variable in an LME model, which included fixed effects for age, sex, and the rate of change in serum NfL and a random intercept term for family. The term of interest was serum NfL rate of change. Models were fit using lme4 in R. See also Supplementary statistical analysis.

#### *Further statistical analyses and models*

Unstandardized regression coefficients (B), standard errors (SE), and p-values from LMEs and linear regression models are reported in figure legends. Statistical analyses mentioned in the figure legends of Extended Data Fig. 2-4 and Supplementary Tables 1 and 2 were conducted with the use of Jmp<sup>®</sup> software, version 13.0 (SAS Institute Inc.). For the analysis of Extended Data Fig. 3c a regression model was created, which approximates the changes of NC and MC. The model uses the rate of change of log serum NfL over EYO. For NC a slightly increasing line over the entire time period was created representing the NfL increase over age. For MC the same development was taken for the very early years until a bifurcation point indicating the divergence of NC and MC. From this point on, MC were shown with a rising slope up to a break of slope, when the line came to a parallel increase as NC. This model uses one common slope at the very beginning, one bifurcation point, and one shift leading to two parallel slopes after symptom onset. See also Supplementary statistical analysis.

## Data availability

Data that support the findings of this study are available from DIAN at <https://dian.wustl.edu/our-research/observational-study/dian-observational-study-investigator-resources/>.

40. Folstein, M.F., Folstein, S.E. & McHugh, P.R. "Mini-mental state". A practical method for grading the cognitive state of patients for the clinician. *Journal of psychiatric research* **12**, 189-198 (1975).
41. Morris, J.C. The Clinical Dementia Rating (CDR): current version and scoring rules. *Neurology* **43**, 2412-2414 (1993).
42. Wechsler, D. *Manual: Wechsler Memory Scale-Revised*, (San Antonio, Texas: Psychological Corporation, 1987).
43. Kuhle, J., *et al.* A comparative study of CSF neurofilament light and heavy chain protein in MS. *Multiple sclerosis (Houndmills, Basingstoke, England)* **19**, 1597-1603 (2013).
44. Disanto, G., *et al.* Serum Neurofilament light: A biomarker of neuronal damage in multiple sclerosis. *Annals of neurology* **81**, 857-870 (2017).
45. Carpenter, B., *et al.* Stan: A Probabilistic Programming Language. *2017* **76**, 32 (2017).
46. Gelman, A., Lee, D. & Guo, J. Stan: A Probabilistic Programming Language for Bayesian Inference and Optimization. *Journal of Educational and Behavioral Statistics* **40**, 530-543 (2015).